,

EVALUATION OF DYNAMIC INERTIA OF TYPE-3 WIND TURBINES

A Project Report

submitted by

AKHIL.S
EE17B151

in partial fulfilment of the

requirements for the award of

the degree of

MASTER OF TECHNOLOGY

under the guidance of

Dr. B. KALYAN KUMAR

DEPARTMENT OF ELECTRICAL ENGINEERING

INDIAN INSTITUTE OF TECHNOLOGY-MADRAS.

JUNE 2022

PROJECT REPORT CERTIFICATE

This is to certify that the project report entitled **Evaluation of Dynamic Inertia of Type-3 Wind Turbines**, submitted by **Akhil.S**, **EE17B151** to the Indian Institute of Technology Madras, for the award of the degree of **Master of Technology** in **Electrical Engineering**, is a bonafide record of project work carried out by him under my supervision and guidance. The contents of the report, in part or in full, have not been submitted to any other institute or university for the award of the any degree.

Place : Chennai
Date :

Dr. B. Kalyan Kumar
Professor
Dept. of Electrical Engineering
IIT- MADRAS, 600036

ACKNOWLEDGEMENTS

This work has been carried out at the Department of Electrical engineering at Indian Institute of Technology Madras.

I would like to express my sincere thanks to my guide, Dr. B. Kalyan Kumar for giving me this project and also for his continuous support, thoughtful guidance and positive words throughout the duration of my work. I could not have wished for a better guide.

I also would like to thank all of my friends, colleagues and hostel mates for cheerful meetings. I would like to thank all the individuals who helped me in my work. I would like to express my thanks for my family for their support and encouragement.

Above all, I thank God for providing strength, protection and guidance throughout my life.

Akhil.S
EE17B151

ABSTRACT

During recent years, the renewable energy development of wind energy has increased rapidly. Due to increasing efficiency of wind turbines, wind energy has developed to become a significant competitor among other sources.

One of the important reasons that led to stability problems for Wind Turbines is low inertia. The decreased inertia is found out to be reason for blackouts too. So, to improve inertia we need to study it based on various other parameters in Wind Turbines. In this work, the modelling and control of Type-3 wind turbine has been discussed and Dynamic inertia for the wind turbine is evaluated on basis of analogy with synchronous generator. The impact of the controllers on inertia is also discussed. The factors that impact inertia are highlighted. This dynamic inertia function is proposed to be much better parameter compared to Inertia constant to determine the dynamic process of inertia and maximize the inertia capacity of type-3 Wind Turbine.

Table of Contents

List of Figures

List of Tables

ABBREVIATIONS

BW	BandWidth
DFIG	Doubly-Fed Induction Generator
MPPT	Maximum Power Point Tracking
PLL	Phase Locked Loop
PWM	Pulse Width Modulation
ROCOF	Rate Of Change Of Frequency
RSC	Rotor Side Converter
SCR	Short Circuit Ratio
SG	Synchronous Generator
WT	Wind Turbine

NOTATIONS

1.	c_{DC}	DC bus capacitor
2.	E_M	Excitation voltage
3.	ω_1	Grid frequency
4.	P_{grid}	Grid power
5.	H	Inertia constant
6.	H_{WT}	Inertia constant of the WT
7.	I_r	Rotor current
8.	I_s	Stator current
9.	L_{line}	Transmission line inductance
10.	P_s	Stator real power
11.	R_s	Stator resistance
12.	V_{DC}	DC link voltage
13.	V_r	Rotor voltage
14.	V_w	Wind speed
15.	X_m	Magnetizing reactance
16.	X_s	Stator reactance

CHAPTER 1

INTRODUCTION

1.1 General

In earlier days, wind power was used to drive boats and ships. Later, people understood that controlling and using alternative renewable energy is the best way to deal with the crisis of energy also considering the pollution of the environment.

Wind energy is one of the renewable energies that controls and uses wind power. Over the years it has been proven as a efficient source of generating electricity with low pollution of atmosphere. It is one of the rapidly increasing sources for generation of electrical power and is expected to grow in the future. Along with gain of energy, the parameters considered for the installation of wind turbines are financial efficiency, environmental effects and effects of grid.

When the penetration level of wind power into power system is lower, the system dynamic behaviour is determined by the synchronous generators present in the power systems. However, if the penetration level of wind power integrated into the grid increases then the behaviour of entire system gets effected. This may lead to stability problems in the power system which further may end in blackouts.

1.2 Cause for stability problems

If the power system is penetrated by a sudden renewable energy the frequency will continue to deteriorate, which may become a potential threat to the power system stability. According to the record of the enormous blackout in south Australia in 2016 it was found out that rate of change of frequency (R.O.C.O.F) attained 6 Hz/s at an initial stage. The cause of the blackout was revealed as low inertia[1].

1.3 Research on Inertia of Type-3 WT

In general the high-scale wind energy equipment installed into grids is identified as the main cause for decreased inertia of the power system. To deal with this problem many researches have put effort to improve the vector control for type-3 wind turbines(WT) but this led to system complexity[2]. Later it was found out that inertial response can be achieved by managing control parameters. But they were not able to reason why inertial response is impacted by control parameters.

It was found out that studying the control parameters and inertial responses of WT was tough as they depend on the model's accuracy and significant amount of simulations. Therefore Inertia constant is proposed to measure the inertia given by type-3 WT when the system undergoes frequency disturbances and this was used mostly for understanding inertia characteristic. However, this method can be only used when the system undergoes any frequency disturbances and it doesn't count the impact of controllers. This method can only measure inertia within a period. So by further studying , the researchers found out that inertial response is not a constant but a transfer function and they determined inertia based on motion model of synchronous generator(SG). However, it was not purely consistent with model of type-3 WT.

1.4 Objectives

This report has the following objectives :

- To provide the basic control and modelling for type-3 WT.
- To highlight the advantages of Dynamic Inertia over Inertia constant
- To derive the transfer function of Dynamic Inertia in analogy with the synchronous generator(SG).
- To present the impact of controllers on Inertia of type-3 WT.

1.5 Report Layout

The organisation of the report is as follows

- Chapter 2 presents a brief overview of how wind turbine works and gives the basic modelling and control of the Type-3 Wind turbine which is used in evaluating the inertia function.

- Chapter 3 gives an understanding on inertia constant and describes the advantages of inertia function over inertia constant. Further it derives the inertia function of the type-3 WT by small signal analysis based on its consistency in power transfer mechanism with synchronous generator.

- Chapter 4 provides the results and analysis of inertia function based on impact of different controllers.

- Chapter 5 gives a brief conclusion and highlights of this work.

CHAPTER 2

TYPE-3 WIND TURBINE

2.1 Wind Turbine

The wind turbine works under the principle of electromagnetic coupling. Basically, it is a device which is used for generating electricity by converting wind's kinetic energy. The huge flow of wind originates the wind power. The aerodynamical forces acting on the turning blades causes the mechanical torque transformation. The shaft of the wind turbine supplies this power to the generator connected with the grid.The block diagram of wind turbine power model is

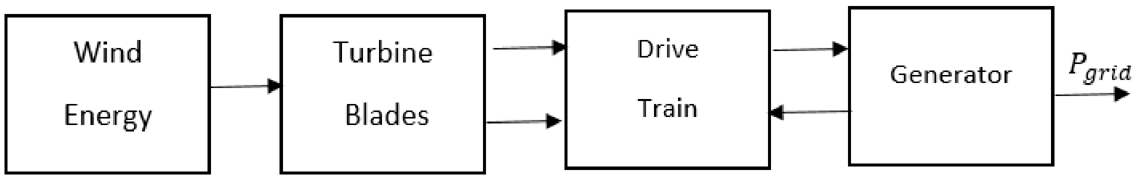

Fig 2.1 : Power extraction from wind turbine

2.2 Control of Type-3 Wind Turbine

The Type-3 Wind turbine(WT) works with the help of Doubly fed induction-generator (DFIG) which is integrated to the grid through large distance transmission lines and a step-up transformer.

As the voltage of the grid will be higher its resistance can be neglected therefore the public grid can be considered equal to Thevenin's equivalent with internal voltage in series with grid inductance.

The synchronization of the grid is done by PLL. The control by voltage and the control by speed is done by using the outer loop (as shown in the Fig 2.2)

The maximum power point tracking curve is used to obtain the reference for the speed control. To ensure the high-quality current of the grid, the current control loop is used and outer loop's output is used for the reference for the current control loop.

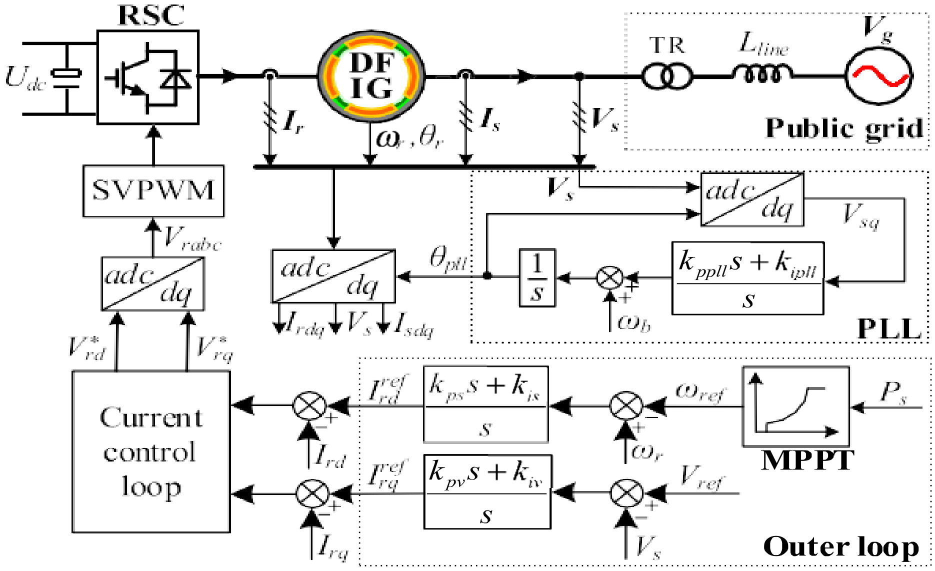

Fig 2.2 : Control block of Type-3 WT

2.3 Modelling of the system

The generator convention is employed by stator vector where as the motion convention is employed by rotor vector. The stator voltage,flux and active power equations can be derived as

$$V_s = -R_s I_s + \frac{d\psi_s}{dt} + j\omega_1 \psi_s \tag{2.1}$$

$$\psi_s = -L_s I_s + L_m I_r \tag{2.2}$$

$$P_s = V_{sd} I_{sd} + V_{sq} I_{sq} \tag{2.3}$$

Since we are neglecting the resistance of stator and by simplifying above equations we get the following equation.

$$P_s = V_{sd} \frac{X_m I_{rd}}{X_s} + V_{sq} \frac{X_m I_{rq}}{X_s} \tag{2.4}$$

Here $X_m = \omega_1 L_m$ is the magnetizing inductance

$X_s = \omega_1 L_s$ is the stator reactance

Where d , q represent d-axis and q-axis components

The rotor side converter is used as the excitation system for type-3 Wind Turbine(WT) therefore the corresponding excitation vector is

$$E_m = jX_m I_r \tag{2.5}$$

Based on this, we can determine the equations (2.1) and (2.3) as following

$$V_s = E_m - jX_s I_s \tag{2.6}$$

$$P_s = \frac{E_m V_s}{X_s} \sin \delta_E \tag{2.7}$$

where $\boldsymbol{\delta_E}$ is the rotor angle (internal) to E_m $and\ V_s$.

From the Fig 2.2 we can determine the relation between grid voltage(public grid) and stator voltage as

$$V_s = V_g + jX_g I_s \tag{2.8}$$

where X_g is the reactance of the grid which implies the transmission line and transformer reactance.

The above equation can be extended with equation (2.6) as

$$V_s = k_{X_s} V_g + k_{X_g} E_m \tag{2.9}$$

where $k_{X_s} = \frac{X_s}{X_s + X_g}$ and $k_{X_g} = \frac{X_g}{X_g + X_s}$

CHAPTER 3

Dynamic Inertia for type-3 Wind turbine

3.1 Comparison between Inertia constant and Dynamic Inertia

Inertia constant is regarded as basic approach to evaluate the inertia in a unit. It is defined as the ratio of rotor kinetic energy to the rated power.

$$H = \frac{J(\Delta\omega_r)^2}{2S_{WT}} \tag{3.1}$$

where J is the moment of inertia of WT, S_{WT} is the WT apparentpower. where as $\Delta\omega_r = \omega_0 - \omega_{min}$ in which ω_0 is the rotor speed at the beginning and ω_{min} is the minimum rotor speed in the period of disturbances of frequency [3].

According to the above equation, it can be analyzed that inertial constant considers two points only in the entire time period to quantify the difference of kinetic energy of the rotor to determine the characteristicsof inertia through out the frequency disturbances. This does not take the process of dynamic adjustment of the power electronic converters. As the minimum speed of the rotor cannot be known before the end of the disturbances, the inertia constant will be calculated only after disturbances.

However, the dynamic inertia provided in this work is aimed towards determining the intrinsic property for type-3 WT. This means to over see the role of combined multiple controllers such as PLL controller, voltage and speed controllers. The dynamic inertia is derived by analogy to the mechanism which is proven to determine the inertia of the synchronous generator.

The dynamic inertia unlike inertia constant varies along with time. Through this dynamic inertia, the dynamic characteristic of inertia process can be determined easily and also effectively determines the impact of controllers on the inertia. More ever, Dynamic inertia helpsto quantify inertia before the frequency disturbances rather than after the disturbances.

The below table shows the comparison between inertia constant and dynamic inertia.

Inertia constant vs Dynamic inertia		
Inertia evaluation method	Inertia constant	Dynamic Inertia
Index feature	constant	Time varying
Object	Rotor speed	Internal controller
Application condition	Evaluates post-disturbance	Evaluates pre-disturbance

Table 3.1: Inertia constant vs dynamic inertia

3.2 Analogy between type-3 Wind Turbine and Synchronous Generator.

The basic equations for voltage and power of Synchronous generator are [4]

$$V_{SG} = E_q - jX_q I_{SG} \quad (3.2)$$

$$P_{SG} = \frac{E_q V_{SG}}{X_q} \sin \delta_{SG} \quad (3.3)$$

According to the equations the equivalent circuit models for type-3 WT and SG which can be integrated into the grid can be attained.

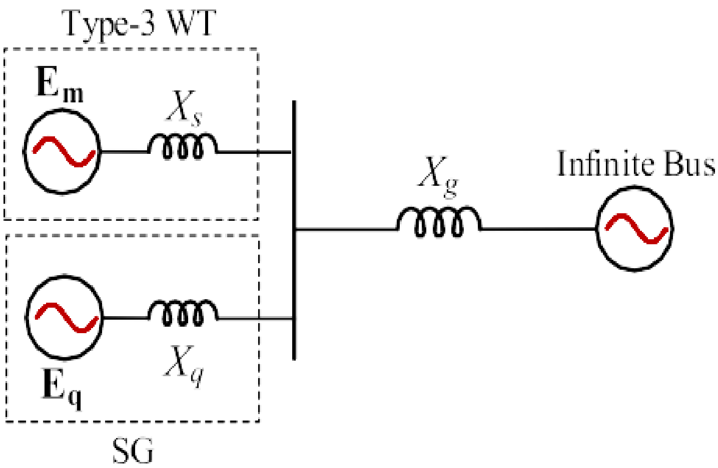

Fig 3.1: Equivalent model for Type-3 WT and SG integrated into grid.

From this model we can analyse that there is some consistency present between the equivalent circuits and mechanisms of power transfer.

From Fig 3.1, we can see that E_q and V_{SG} OF SG correspond to E_m and V_s OF WT . The internal angle δ_{SG} corresponds to δ_E and θ_{SG} of E_q corresponds to θ_E of E_m.

Though there are many similarities between type-3 WT and the SG models, some differences exist too. Because of the effect of governor the rotor always maintains rated speed and also SG shows the supremacy on the grid. However, The type-3 WT is not very efficient in adapting to change in conditions of the grid.

The phase locked loop(PLL) is the only way to detect the disturbance in the frequency . This means that if disturbances of frequency occur in the model the corresponding deviation will be realized by the PLL and then converts the deviation to a phase angle. If the phase angle changes dynamically then the internal rotor angle and electromagnetic power will vary corresponding to it as the calculation of power is based on the phase angle. Therefore one must consider the dynamics of PLL when electromagnetic power is analyzed during frequency disturbances.

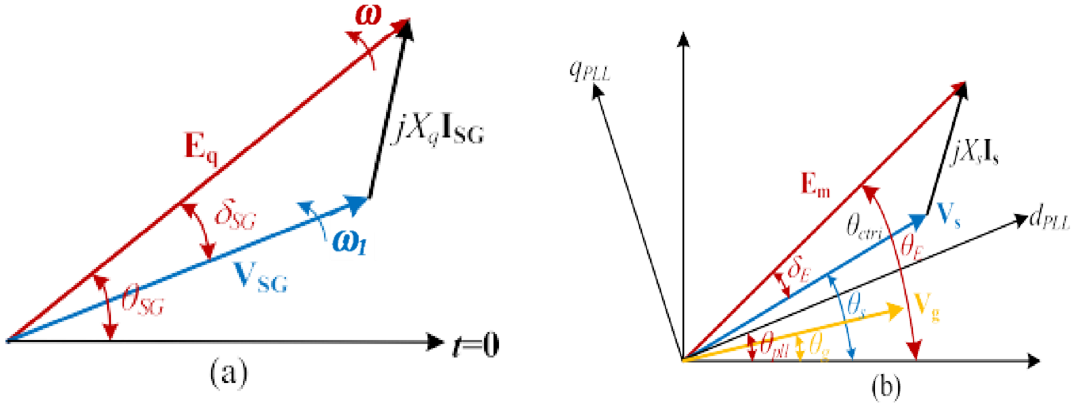

Fig 3.2 : (a)SG (b) Type-3 WT

3.3 Inertia of Synchronous generator.

To determine the inertia of type-3 WT, we need to study the inertia of the SG.When imbalances in the power occur the response of inertia is generally exposed in accordance with the swing equations

$$J\frac{d\Delta\omega}{dt} = P_m - P_e \quad (3.4)$$

$$\frac{d^2\delta}{dt^2} = \frac{d^2\theta}{dt^2} = \frac{d\Delta\omega}{dt} \quad (3.5)$$

3.4 Inertia of Type-3 Wind Turbine

The following assumptions are made throughout this model.

- The transient dynamics of current and flux are not taken into consideration as the work analyses characteristic of inertia in WT which is a issue of long term and can be classified into electromechanical timescale.
- While disturbances of frequency occur the wind speed is maintained to be constant

Keep note that following model analysis is done in PLL synchronous frame(i.e synchronous reference frame)

3.4.1 Small signal analysis on Electrical part

The derivation of Inertia of WT is based on analogy with Inertia of SG. The small signal analysis of the mechanical and electrical parts will be performed to get the transfer function of inertia.

The small signal equation for the active power will be calculated from

$$\Delta P_e = k_{Em}\Delta E_m + k_{Vs}\Delta V_s + k_{\delta E}\Delta\delta_E \qquad (3.6)$$

where k_{Em} is the coefficient of excitation and k_{Vs} is the coefficient of terminal voltage and $k_{\delta E}$ is the coefficient of synchronous power.

Firstly, In the PLL synchronous reference frame the excitation vector in scalar form can be expressed as

$$E_m = \sqrt{E_{md}^2 + E_{mq}^2} \qquad (3.7)$$

$$\theta_{ctrl} = arctan\frac{E_{mq}}{E_{md}} \tag{3.8}$$

The small signal equations for ΔE_m and$\Delta\theta_{ctrl}$ are

$$\Delta E_m = \frac{E_{md0}}{E_{m0}}\Delta E_{md} + \frac{E_{mq0}}{E_{m0}}\Delta E_{mq} \tag{3.9}$$

$$\Delta\theta_{ctrl} = \frac{E_{md0}}{E_{m0}^2}\Delta E_{mq} - \frac{E_{mq0}}{E_{m0}^2}\Delta E_{md} \tag{3.10}$$

Similarly, the expressions for amplitude and phase of terminal voltage can be achieved as

$$\Delta V_s = \frac{V_{sd0}}{V_{s0}}\Delta V_{sd} + \frac{V_{sq0}}{V_{s0}}\Delta V_{sq} = \Delta V_{sd} \tag{3.11}$$

$$\Delta\theta_s - \Delta\theta_{pll} = \frac{V_{sd0}}{V_{s0}^2}\Delta V_{sq} - \frac{V_{sq0}}{V_{s0}^2}\Delta V_{sd} = \frac{V_{sd0}}{V_{s0}^2}\Delta V_{sd} \tag{3.12}$$

By grid voltage and stator voltage relation and above equation thefollowing can be attained.

$$\Delta V_s = \Delta V_{sd} = k_{X_s}\Delta V_{gd} + k_{X_g}\Delta E_{md} \tag{3.13}$$

The d-axis component and phase of voltage vector of the grid can be expressed as

$$V_{gd} = V_g \cos(\theta_g - \theta_{pll}) \quad (3.14)$$

$$\theta_g = \theta_{pll} + arctan \frac{V_{sq} - k_{X_g} E_{mq}}{V_{sd} - k_{X_g} E_{md}} \quad (3.15)$$

here θ_{pll} is phase angle calculated by PLL

The small signal expressions for above parameters by considering V_g as constant are

$$\Delta V_{gd} = \cos(\theta_{g0} - \theta_{pll0})\Delta V_g - V_{g0} \sin(\theta_{g0} - \theta_{pll0}) \times (\theta_{g0} - \theta_{pll0})$$

$$= -V_{g0} \sin(\theta_{g0} - \theta_{pll0}) \times (\theta_{g0} - \theta_{pll0}) = k_g(\theta_{g0} - \theta_{pll0})$$

(3.16)

$$\Delta\theta_g = \Delta\theta_{pll} + k_{\theta gsq}(\theta_s - \theta_{pll}) - k_{\theta g E_{mq}} \Delta E_{mq} - k_{\theta g E_{md}} \Delta E_{md} + k_{\theta gsd} \Delta$$

(3.17)

By substituting the equation 3.16 into 3.13 the following result is obtained

$$\Delta V_s = k_g k_{Xs} \left(k_{\theta gsq} \left(\Delta\theta_s - \Delta\theta_{pll}\right) - k_{\theta gEmq} \Delta E_{mq} - k_{\theta gEmd} \Delta E_{md} + k_{\theta gsd} \Delta V_s\right) + k_{Xg} \Delta E_{md}$$

(3.18)

According to the Fig 3.2 (b) $\Delta\delta_E$ can be derived as

$$\Delta\delta_E = \Delta\theta_E - \Delta\theta_s = \Delta\theta_{ctrl} + \Delta\theta_{pll} - \Delta\theta_s \quad (3.19)$$

The small signal model of PLL according to [5] is

$$G_{pll}(s) = \frac{\Delta\theta_{pll}(s)}{\Delta\theta_s(s)} = \frac{k_{ppll}s+k_{ppll}}{s^2+k_{ppll}s+k_{ppll}} \qquad (3.20)$$

where k_{ppll} is proportional gain and k_{ipll} is integral gain of the controller

Through these equations, the small signal model for electrical part under imbalances of power is derived. We can also understand the impacts of internal angle, terminal voltage and excitation voltage on the electromagnetic power. We can also find the other factors effecting these parameters. We can understand how the basic angle for the type-3 WT can be obtained. The excitation voltages (both d-axis and q-axis) is the important interface to make a link between internal control and external condition for type-3 WT's.

As the reference for the rotor is obtained from MPPT curve the reference for speed can be considered as constant [6].

$$\Delta E_{md} = \frac{k_{ps}s+ k_{is}}{s} X_m(\Delta\omega_r - \Delta\omega_{ref}) \quad = G_{PIs}(s)X_m\Delta w_r \qquad (3.21)$$

$$\Delta E_{mq} = \frac{k_{pv}s+ k_{iv}}{s} X_m(\Delta V_{ref} - \Delta V_r) \quad = G_{PIv}(s)X_m\Delta V_r \qquad (3.22)$$

Where k_{is} and k_{ps} are integral and proportional gains of the speed controller and k_{iv} and k_{pv} are integral and proportional gains of voltage controller.

3.4.2 Small signal analysis on Mechanical part

The small signal model for mechanical part type-3 WT can be obtained as

$$\Delta P_m - \Delta P_e = 2H\omega_{r0} s \Delta w_r \qquad (3.23)$$

We have now achieved small signal model for type-3 WT under imbalances of power for both electrical and mechanical part. By further simplification we get the model similar to SG as shown in the fig 3.3.

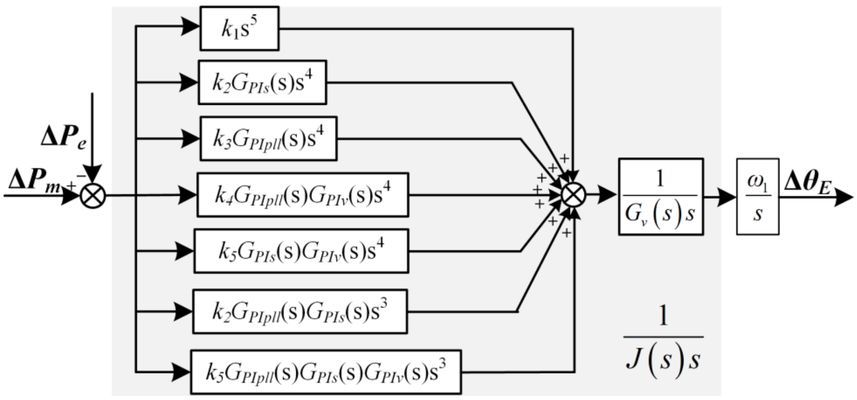

Fig 3.3 : Phase motion model of type-3 WT

Finally the Inertia transfer function J(s) can be expressed as $G_v(s)/\mathrm{D(s)}$.Where

$$G_v(s) = (\omega_1(1 - k_g k_{Xs}(k_{\theta gsd} + k_{\theta gsd} k_{eq} V_s) + (k_{\theta gEmd} k_g k_{Xs} - k_{Xg}) X_m G_{PIv}(s))s^3) \qquad (3.24)$$

$$D(s) = k_1 s^5 + (k_2 G_{PIs}(s) + k_3 G_{PIpll}(s)) s^4 + \left(k_4 G_{PIpll}(s) + k_5 G_{PIs}(s)\right) G_{PIv}(s)\, s^4 + (k_2 + k_5 G_{PIs}(s)) G_{PIpll}(s) G_{PIv}(s)\, s^3 \tag{3.25}$$

All the constants mentioned above are described in the Appendix 1.

As we have derived we can now see that Inertia for type-3 WT is a transfer function rather than a constant like SG. We can also find out that inertia is dependent on various parameters like internal controllers,voltage controller, speed and PLL controllers also. It also depends on external strength of grid. If grid is very strong then the angle between stator and grid voltage can be considered as zero, therefore k_g becomes zero and in turn k_1 also becomes zero. In this case the remaining constants gives us the understanding of impact of controllers.

CHAPTER 4

Results and Analysis of Inertia of Type-3 Wind Turbine

4.1 Reference Frame

In this chapter, we will analyse the impact of parameters that impact the inertia of type-3 WT based on the transfer function we obtained from the above chapter. Firstly, note that this analysis is donein synchronous reference frame. That indicates that the frequency in the static reference frame will get transformed to zero(Hz) in the synchronous reference frame.

4.2 Impact of inertia by PLL controller

Generally, the design of PLL controller is made by keeping targets as bandwidths and damping factors[7]. The parameters of the PLL controller under various bandwidths and damping factors are described in the Table 4.1.

BW / ξ	13.32 Hz		8Hz		0.6Hz		0.42Hz	
	k_{ppll}	k_{ipll}	k_{ppll}	k_{ipll}	k_{ppll}	k_{ipll}	k_{ppll}	k_{ipll}
0.8	60	1400	35.7	498	2.67	2.8	1.89	1.4
0.5	43.6	1901	26	676	1.94	3.8	1.38	1.9
0.3	28.7	2281	17.2	823	1.29	4.6	0.9	2.3

Table 4.1 PLL parameters

The figures (4.1) –(4.4), describes the impact of PLL controller on the 1.5 MW type-3 WT. The parameters of the WT are provided in the Table 4.2.

Symbol	Description	Value
P_N	Rated power	1.5MW
U_{gl}	Grid line voltage	690V
f_g	Grid frequency	50Hz
U_{dc}	DC link voltage	1200V
U_{rN}	Rated rotor voltage	2350V
R_s	Stator resistance	0.023 p.u
R_r	Rotor resistance	0.016 p.u.
L_m	Magnetizing inductance	2.9 p.u.
L_{ls}	Stator leakage inductance	0.18 p.u.
L_{lr}	Rotor leakage inductance	0.16 p.u.
C_{dc}	DC bus capacitor	10000 F
H	Inertia constant	0.685 s
H_{wt}	Inertia constant of wind turbine	4.32 s
$K_{ps,}K_{is}$	Speed PI controller	3,0.6
$K_{pv,}K_{iv}$	Voltage controller	-3,-50
$K_{pi,}K_{ii}$	Rotor side current PI controller	0.6,8
$K_{ppll,}K_{ipll}$	PLL controller	1.89,1.4
V_w	Wind speed	10m/s
SCR	Short circuit ratio	2

Table 4.2 : 1.5 MW WT parameters

The Inertia is predominantly found in the beginning of the deviation of the frequency. As the deviation increases, the inertia is significantly reduced and even becomes zero. As the goal of control of inertia is to decrease the starting Rate of change of frequency(R.O.C.O.F) during the disturbances of the frequency this gets along with the expectation. Therefore, in this work we are going to understand the impact of different controllers by analysing increasing part of the inertia.

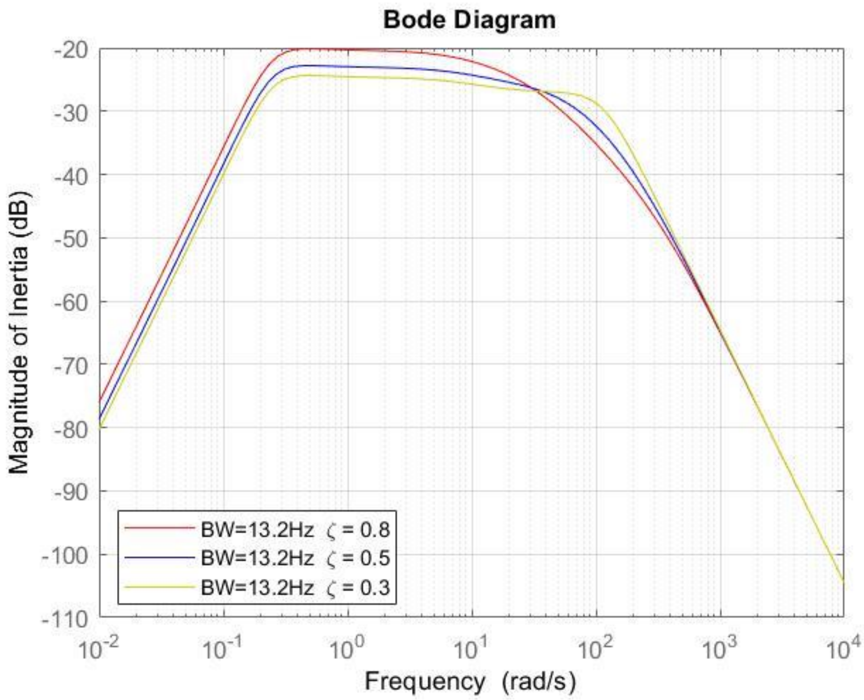

Fig 4.1 : Inertia for BW = 13.2 Hz

4.2.1 Inertia at BW= 13.2 Hz

The Fig 4.1 gives the inertia at higher bandwidth i.e (13.2 Hz) and different damping factors. It is found that magnitude of inertia is almost equal to 0 (less than 0.1 in absolute scale). This analyses that the type-3 WT does not supply any inertia to the grid.

As for the damping factor is concerned, it is found that as the damping factor increases the magnitude of inertia is found to be higher compared to the lower damping factors. This means that more inertia is provided to the grid with higher damping factors

Therefore, at Bandwidth= 13.2 Hz it is found that very low inertia is supplied to the grid and a higher damping factor at this bandwidth suggests better inertia to the grid.

4.2.2 Inertia at BW= 8 Hz

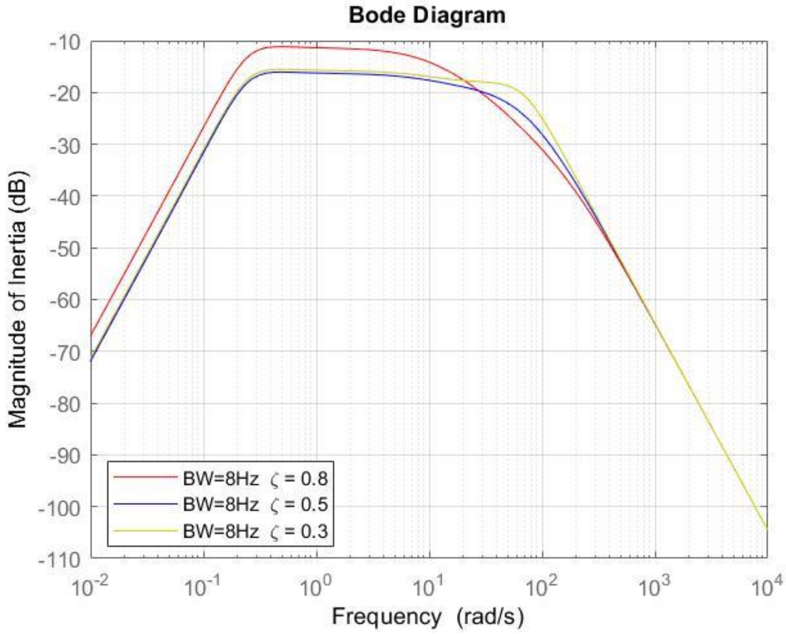

Fig 4.2: Inertia for BW= 8 Hz

Fig 4.2 gives the magnitude of inertia at Band Width BW= 8 Hz and different damping factors. Though it's magnitude is comparatively better to that at higher band width (13.2 Hz). it's magnitude is still closer to zero (less than 0.3 in abs scale) and it does not supply good inertia to grid.

As for the damping factors at 8 Hz are concerned, Higher damping factors have better magnitude compared to the lower ones. That strengthens that higher damping factors provide better inertia to the grid.

Now we have seen the fast PLL responses of the inertia at 13.2 Hz and 8 Hz. We can strongly point out that inertia provided to the grid is negligible, but higher damping factors have shown better inertia though the difference is small.

4.2.3 Inertia at BW= 0.6 Hz

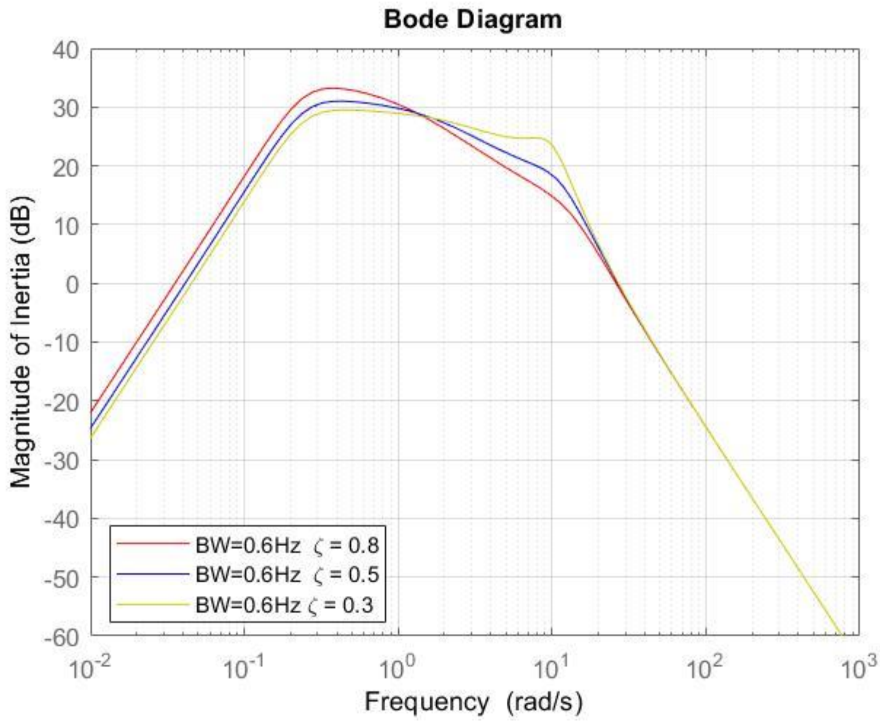

Fig 4.3: Inertia for BW= 0.6 Hz

Fig 4.3 gives the frequency deviation curve of inertia at BW= 0.6Hz and other damping factors. Unlike to higher band width cases, magnitude at this bandwidth(0.6 Hz) is found to be remarkably high.This magnitude of inertia is much higher than that of general inertia constants of normal generators (less than 10 s). The WT provides larger inertia to the grids.

As for the damping factors are concerned, Higher damping factor provides better inertia at this band width also. In this case damping factors are also considered as decent factors as the magnitude of inertia for higher damping factor is much higher when compared to lower damping factor according to the above figure.

4.2.4 Inertia at BW= 0.42 Hz

The Fig 4.4 gives the frequency deviation curve of inertia at BW= 0.42Hz and other damping factors. Magnitude at this bandwidth(0.42 Hz) is found to be higher than the previous case. This suggests even more inertia to the grid.

As for the damping factors are concerned, Higher damping factor provides better inertia at this band width also.

4.2.5 Highlights of PLL responses

After analysing all the PLL responses we can conclude that the slowPLL responses (low band width) are found out to be significantly efficient in providing inertia to the grids. The fast PLL responses hardly provide any inertia to the grid. The higher damping factors are proven to be better for supplying inertia.

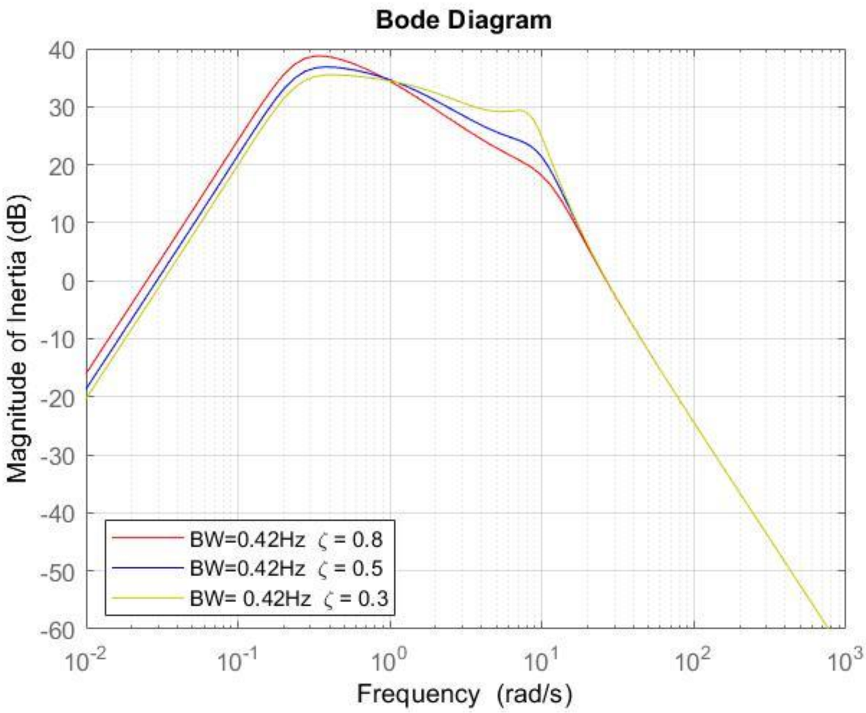

Fig 4.4 : Inertia for BW= 0.42 Hz

4.3 Impact of speed and voltage controllers on Inertia

From the previous section we have found out that slow PLL responses(low bandwidth) are efficient in providing inertia for the grid. So, we are going to do the analysis of speed controllers and voltage controllers by taking the slow PLL response parameters. (BW=0.42 Hz, ζ = 0.8,k_{ps}= 3, k_{is}=0.6, k_{pv}=-3, k_{iv}=-50, SCR=2).

4.3.1 Impact of proportional gain of speed controller on Inertia

Fig 4.5 gives the frequency deviation curve of inertia at different proportional gains of the speed controller.

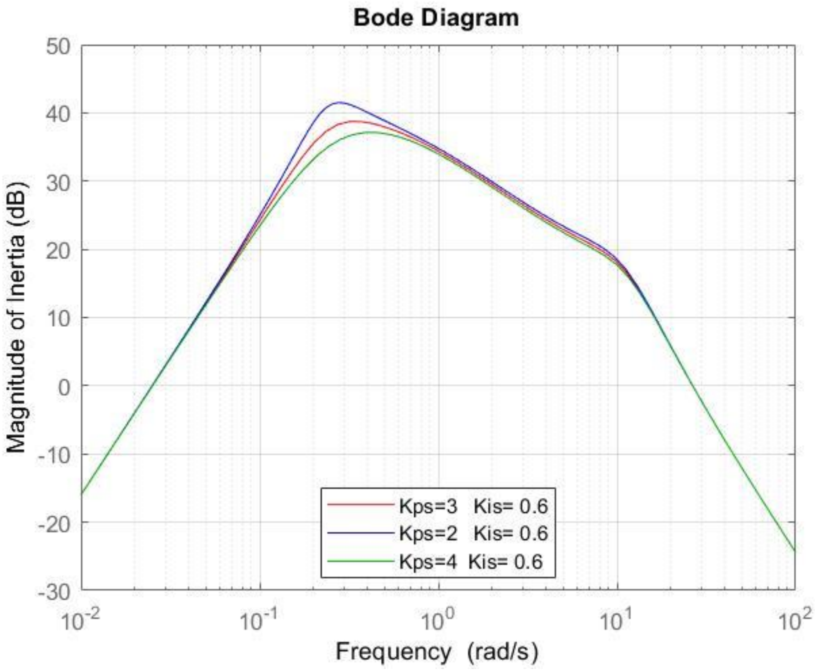

Fig 4.5 : proportional gain of Speed controller impact on Inertia

It is found out that as the proportional gain of the speed controller increases the inertia is greatly decreased.

4.3.2 Impact of integral gain of speed controlleron Inertia

The Fig 4.6 gives the frequency deviation curve of inertia at different integral gains of the speed controller.

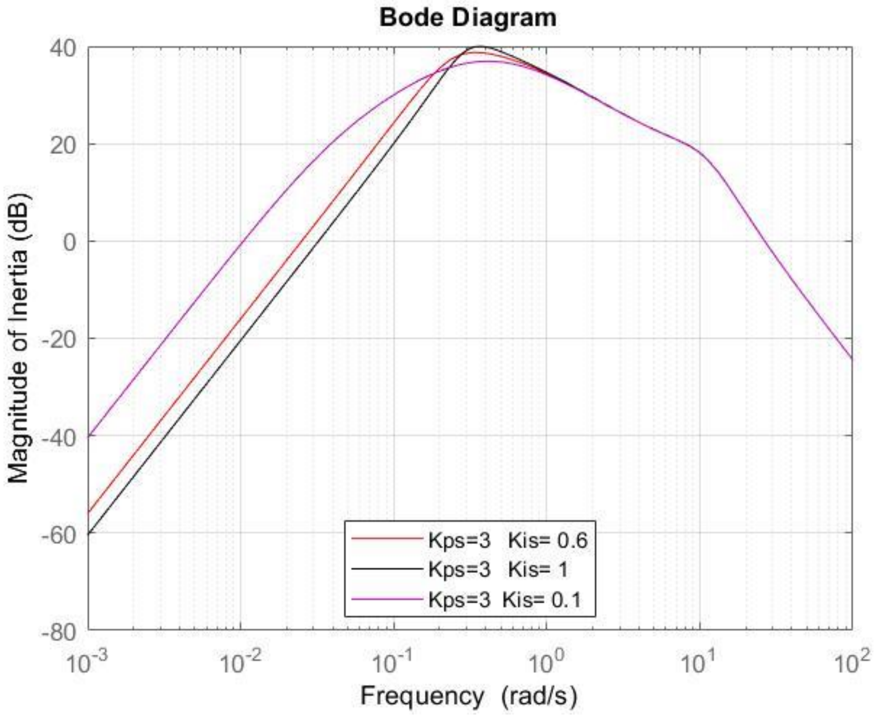

Fig 4.6: Integral gain of Speed controller impact on Inertia

We can see that for a short duration during the initial frequency disturbances, better inertia was given by low integral gain of the speed controller, however after some time high integral gain provides better inertia contribution.

4.3.3 Impact of proportional gain of voltage controller on Inertia

The Fig 4.7 gives the frequency deviation curve of inertia at different proportional gains of the voltage controller. As we can see even after

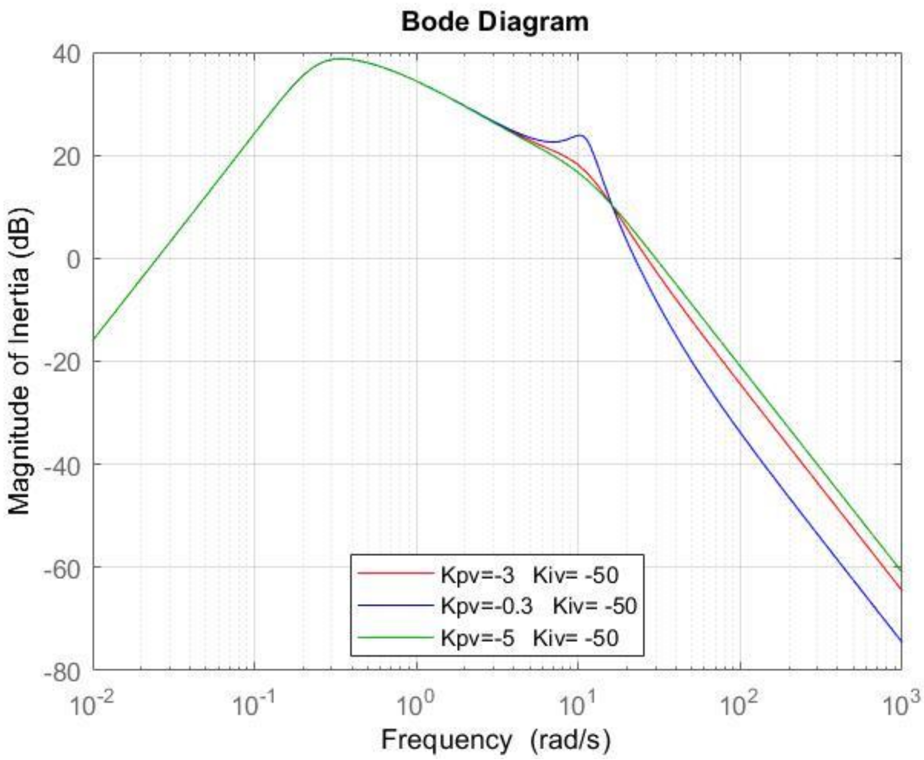

Fig 4.7 : Proportional gain of voltage controller impact on Inertia

increasing and decreasing the proportional gain of the voltage controller by a big range, there is no much change in the inertia. Therefore, proportional gain cannot impact inertia.

4.3.4 Impact of integral gain of voltage controlleron Inertia

The Fig 4.8 gives the frequency deviation curve of inertia at different integral gains of the speed controller. As we can see, there is only change

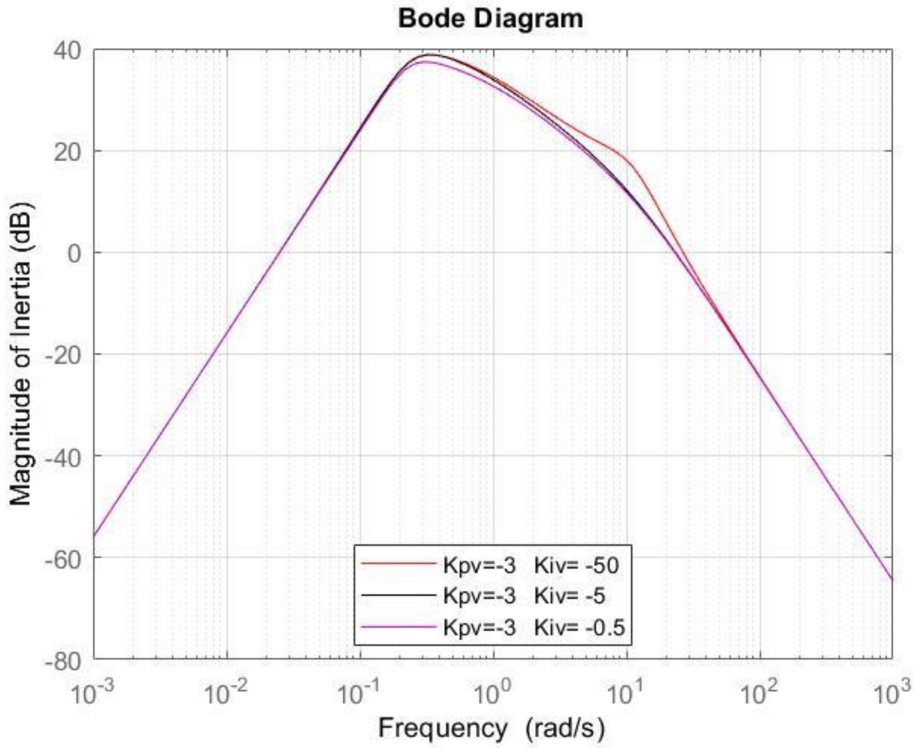

Fig 4.8 : Integral gain of voltage controller impact on Inertia

in inertia if the integral gain of voltage controller is largely decreased. However, the inertia is decreased in that case. So there is no use in changing integral gain of the voltage controller.

4.3.5 Highlights of impact of voltage and speed controllers on inertia

It is found out that high proportional gain of the speed controller decreases inertia. The low integral gain of the speed controller provides better inertia during initial disturbances but later high integral gain provides better,where as for voltage controllers, there is no much useful impact on the inertia.

CHAPTER 5

Conclusion

In this work the modelling and control of type-3 wind Turbine (WT) is discussed. The advantages on the inertia function over inertia constant has been highlighted. The derivation of Inertia function is derived based on analogy of consistent power transfer mechanisms between type-3 WT and synchronous generator (SG) integrated to the grid.

Then an analysis on inertia is provided based on the transfer function derived. The impacts of various controllers like voltage, speed and PLL controllers have been displayed. It is found out that inertia is majorly impacted by PLL controller. The lower bandwidth of PLL controller accounts for significantly higher inertia compared to the higher bandwidth. The higher damping factors add an additional magnitude to the inertia. As for the speed controllers, higher proportional gain decreases the inertia and though the lower integral gain provides better inertia during the initial disturbances of frequency, higher integral gain provides better inertia at a later time. Even though the proportional gain of the voltage controller is varied largely, only little impact is made in controllers. The integral gain of the voltage controllers shows no much useful impact on inertia.

APPENDIX – 1

$$k_{Vs} = \frac{E_{m0}}{X_s} sin\,\delta_{E0}$$

$$k_{Em} = \frac{V_{s0}}{X_s} sin\,\delta_{E0}$$

$$k_{\delta E} = \frac{E_{s0}V_{s0}}{X_s} cos\,\delta_0$$

$$k_{Emd} = \frac{E_{md0}}{E_{m0}}\frac{V_{s0}}{X_s} sin\,\delta_{E0}$$

$$k_{Emq} = \frac{E_{mq0}}{E_{m0}}\frac{V_{s0}}{X_s} sin\,\delta_{E0}$$

$$k_{\theta gsd} = \frac{X_g(X_s+X_g)E_{mq0}}{\left((X_s+X_g)V_{sd0}-X_gE_{md0}\right)^2+(X_gE_{mq0})^2}$$

$$k_{\theta gsq} = \frac{(X_s+X_g)V_{s0}\left((X_s+X_g)V_{sd0}-X_gE_{md0}\right)}{\left((X_s+X_g)V_{sd0}-X_gE_{md0}\right)^2+(X_gE_{mq0})^2}$$

$$k_{g\theta Emd} = \frac{X_g^2E_{mq0}}{\left((X_s+X_g)V_{sd0}-X_gE_{md0}\right)^2+(X_gE_{mq0})^2}$$

$$k_{g\theta Emq} = \frac{X_g\left((X_s+X_g)V_{sd0}-X_gE_{md0}\right)}{\left((X_s+X_g)V_{sd0}-X_gE_{md0}\right)^2+(X_gE_{mq0})^2}$$

$$k_{eqmd} = \frac{K_{Emd}}{k_{\delta E}} + k_{\theta cd}$$

$$k_{eqmq} = \frac{K_{Emq}}{k_{\delta E}} + k_{\theta cq}$$

$$k_{eqvs} = \frac{K_{Vs}}{k_{\delta E}}$$

$$k_1 = \frac{k_{\theta gsq} k_g k_{Xs} k_{\theta gsd}}{k_{\delta E}}$$

$$k_2 = \frac{X_m}{2H\omega_{r0}} \left(k_{eqmq} - k_g k_{Xs} \left(k_{eqmq} k_{\theta gsd} + k_{\theta gEmq} k_{eqvs} \right) \right)$$

$$k_3 = \frac{1 - k_g k_{Xs} k_{\theta gsd}}{k_{\delta E}}$$

$$k_4 = \frac{X_m (k_{\theta gEmd} k_g k_{Xs} - k_{Xg})}{k_{\delta E}}$$

$$k_5 = \frac{X_m^2}{2H\omega_{r0}} k_{eqmq} \left(k_{\theta gEmd} k_g k_{Xs} - k_{Xg} \right)$$

References

1. Australian Energy Market Operator. (2017). Black System South Australia 28 September 2016 Third Preliminary Report. [Online].

2. J. Morren, S. W. H. De Haan, W. L. Kling, and J. A. Ferreira, "Wind turbines emulating inertia and supporting primary frequency control," IEEE Trans. Power Syst., vol. 21, no. 1, pp. 433–434, Feb. 2006

3. J. Ekanayake and N. Jenkins, "Comparison of the response of doubly fed and fixed-speed induction generator wind turbines to changes in network frequency," IEEE Trans. Energy Convers., vol. 19, no. 4, pp. 800–802, Dec. 2004.

4. P. Kundur, Power System Stability and Control. New York, NY, USA: McGraw-Hill, 1994

5. B. Wen, D. Boroyevich, R. Burgos, P. Mattavelli, and Z. Shen, "Analysis of DQ small-signal impedance of grid-tied inverters," IEEE Trans. Power Electron., vol. 31, no. 1, pp. 675–687, Jan. 2016

6. K. Clark, N. W. Miller, and J. J. Sanchez-Gasca, "Modeling of GE wind turbine-generators for grid studies, version 4.5," GE Int., Inc., Schenectady, NY, USA, Tech. Rep., Apr. 2010. [Online].

7. V. Kaura and V. Blasko, "Operation of a phase locked loop system under distorted utility conditions," IEEE Trans. Ind. Appl., vol. 33, no. 1, pp. 58–63, Jan. 1997.